Available online at www.sciencedirect.com
ScienceDirect
European Journal of Pharmaceutics and Biopharmaceutics 69 (2008) 117–125
European Journal of Pharmaceutics and Biopharmaceutics
www.elsevier.com/locate/ejpb

Research paper

Cellular uptake and cytotoxicity of shell crosslinked stearic acid-grafted chitosan oligosaccharide micelles encapsulating doxorubicin

Fu-Qiang Hu *, Xiu-ling Wu, Yong-Zhong Du, Jian You, Hong Yuan *

College of Pharmaceutical Science, Zhejiang University, Hangzhou, PR China

Received 16 July 2007; accepted in revised form 27 September 2007
Available online 5 October 2007

Abstract

Stearic acid-grafted chitosan oligosaccharide (CSO-SA) with 3.48% amino-substituted degree (SD%) was synthesized by coupling reaction. The CSO-SA could self-aggregate to form micelle with a critical micelle concentration (CMC) at 0.035 mg/mL in the aqueous phase. The CSO-SA self-aggregate micelles indicated spatial structure with multi-hydrophobic core. One CSO-SA chain could form 2.8 hydrophobic cores. Cellular uptakes of CSO-SA micelles by using A549, LLC, and SKOV3 cells as model tumor cell lines showed the faster cellular internalization of CSO-SA micelles, and the cellular uptakes on the LLC and SKOV3 cells were higher than that on the A549 cells. Doxorubicin (DOX) was then used as a model drug to incorporate into CSO-SA micelles. To reduce the initial burst drug release from CSO-SA micelles loading DOX (CSO-SA/DOX), the shell of CSO-SA micelles was crosslinked by glutaraldehyde. The shell crosslinking of CSO-SA micelles reduced the micelle size and surface potential, but it did not significantly affect the cellular uptake and drug encapsulation efficiency of CSO-SA micelles. The cellular inhibition experiments demonstrated that the cytotoxicity of DOX was increased by the encapsulation of CSO-SA micelles. CSO-SA/DOX displayed the best antitumor efficacy in SKOV3 cell line due to the higher cellular uptake percentage of CSO-SA micelles and the lower sensitivity of free drug to the cells. The cytotoxicities of shell crosslinked CSO-SA/DOX were highly enhanced in all cell lines than those of unmodified CSO-SA/DOX.

Keywords: Stearic acid; Chitosan oligosaccharide; Polymeric micelle; Crosslink; Cellular uptake; Cytotoxicity

1. Introduction

During the past decade there has been a growing interest in the investigation of polymeric micelles as a potential carrier for anticancer drug delivery [1]. Polymeric micelles have a core–shell structure composed of hydrophobic segments as the internal core and hydrophilic segments as a surrounding corona in aqueous medium. The internal hydrophobic core provides a storeroom for loading hydrophobic drug. The hydrophilic shell allows to retain the stability of polymeric micelle in aqueous environment, and the active targeting to tumor cells by further modification [2–5]. The nanoscale dimensions of polymeric micelles permit the efficient accumulation in tumor tissue via the enhanced permeability and retention (EPR) effect, which is termed as passive targeting [6,7].

Comparing with traditional micelles of low-molecular-weight surfactant, polymer micelles are generally more stable with a relatively lower CMC, and show slower dissociation and enhanced stabilization in aqueous environment [8]. However, polymer micelles are a dynamic system, the shell of the core–shell architecture serving as a membrane-like layer to gate transport of drug into and out of the core domain [9]. In fact, interactions between drug and core domain of polymeric micelles rely on the delicate balance of relatively weak interactions, such as hydrophobic, hydrogen-bonding, and electrostatic [10], so polymer micelles have a limitation as a drug delivery system because they disintegrate after dilution by the body fluids, bringing initial burst drug release. There is evidence that polymer

* Corresponding authors. College of Pharmaceutical Science, Zhejiang University, 388 Yuhangtang Road, Hangzhou 310058, PR China. Tel.: +86 571 88208441; fax: +86 571 88208439.
E-mail addresses: hufq@zju.edu.cn (F.-Q. Hu), yuanhong70@zju.edu.cn (H. Yuan).

0939-6411/$ - see front matter © 2007 Elsevier B.V. All rights reserved.
doi:10.1016/j.ejpb.2007.09.018

micelle structure can be reinforced by the formation of crosslinks at surface [11].

Chitosan is a natural polysaccharide derived from chitin by alkaline deacetylation and consists of 2-amino-2-deoxy-(1–4β)-D-glucopyranose residues (D-glucosamine units) and *N*-acetyl-D-glucosamine units [12]. It was generally regarded as non-toxic, biocompatible and biodegradable, and was widely accepted as material of drug delivery carriers. In recent years, many researchers focused on the water-soluble chitosan with lower molecular weight, chitosan oligosaccharide (CSO), to synthesize the chitosan oligosaccharide hydrophobic derivatives for the controlled release of hydrophobic antitumor drug [13–15]. In our previous researches, the chitosan oligosaccharide hydrophobic derivatives CSO-SA, was synthesized by the coupling reaction in the presence of 1-ethyl-3-(3-dimethylaminopropyl) carbodiimide (EDC) [16]. The chemical conjugate of CSO-SA could self-aggregate to form micelles with a lower CMC in the aqueous phase. The micelle size was affected by micelle concentration, pH value, and ion concentration of medium. The CSO-SA micelles had the positive surface charge, and could compact plasmid DNA to form micelle/DNA complex nanoparticles, which showed higher *in vitro* gene transfection efficiency [17]. The hydrophobic cores of CSO-SA micelles could load the hydrophobic antitumor drug, paclitaxel, and the drug release from CSO-SA micelles was adjusted by the shell crosslink of CSO-SA [18]. Further studies found that the CSO-SA micelles had spatial structure with multi-hydrophobic core, and could be rapidly uptaken by tumor cells [19].

Doxorubicin is one of the most useful antibiotics with a wide spectrum of activity against malignancy, such as, lung cancer, haematological malignancies, breast cancer, and so on. Although it is also used for treating other tumors like ovarian carcinoma, liver cancer, and stomach cancer, it is not the first selection in the clinic because of its lower sensitivity against these cells [20–22]. To improve the antitumor activity and reduce the side effects of doxorubicin, many polymeric micelle delivery systems of doxorubicin were developed [23–25].

In this paper, using doxorubicin as a model antitumor drug, human lung carcinoma epithelial cell (A549), Lewis lung carcinoma cell (LLC), and human ovarian cancer cell line (SKOV3) as model tumor cells, the effects of shell crosslinking of CSO-SA micelle on the cellular uptake of shell crosslinked CSO-SA micelles and the cytotoxicity of shell crosslinked CSO-SA micelles loading doxorubicin were investigated in detail, comparing with those of unmodified CSO-SA micelles and CSO-SA micelles loading doxorubicin.

2. Materials and methods

2.1. Materials

Chitosan oligosaccharide (CSO) with about 15.0 kDa weight average molecular weight was obtained by enzymatic degradation of 95% deacetylated chitosan ($M_w = 45.0$ kDa), which was supplied by Yuhuan Marine Biochemistry Co., Ltd., Zhejiang, China [16–19]. 1-Ethyl-3-(3-dimethylaminopropyl) carbodiimide (EDC) and 2,4,6-trinitrobenzene sulfonic acid (TNBS) were purchased from Sigma Chemical Co., St. Louis, USA. Pyrene was purchased from Aldrich Chemical Co., USA. 1-Dodecylpyridinium chloride (DPC) was purchased from Chemical Industries Co., Ltd., Japan. Glutaraldehyde (25%) was purchased from Wulian Chemical Plant, China. Stearic acid was purchased from Chemical Reagent Co., Ltd., Shanghai China. Doxorubicin·HCl (DOX·HCl) was gifted by Xingchang Pharmacy Co., Ltd., Zhejiang, China. Dimethyl sulfoxide (DMSO) was purchased from Haishuo Biochemistry Co., Ltd., Wuxi, China. Glycine was purchased from Kangjian Biochemistry Co., Ltd., Shanghai, China. A549, LLC, and SKOV3 cell lines were purchased from Institute of Biochemistry and Cell Biology, Shanghai, China. Dulbecco's modified Eagle's medium (DMEM) and trypsin–EDTA were purchased from Gibco-BRL, MD, USA. Fetal bovine serum (FBS) was purchased from Sijiqing Biologic Co., Ltd., Zhejiang, China. 3-(4,5-Dimethyl-thiazol-2-yl)-2,5-diphenyl-tetrazolium bromide (MTT) was purchased from Sigma Chemical Co., St. Louis, USA. All other solvents were of analytical or chromatographic grade.

2.2. Synthesis of CSO-SA

The chemical conjugate of CSO-SA was synthesized by the coupling reaction of carboxyl group of SA with amine group of CSO in the presence of 1-ethyl-3-(3-dimethylaminopropyl) carbodiimide (EDC) [26]. Briefly, 100 mg CSO was dissolved in 20 mL deionized water (DI water), and 8 mg stearic acid was dissolved in 10 mL hot ethanol, respectively. They were then mixed at 80 °C under stirring. After 10 mg EDC was added into the mixture, the coupling reaction was carried out for 5 h at 80 °C under stirring with 250 rpm. After the reaction, the reaction solution was dialyzed against 10% ethanol solution using a dialysis membrane (MWCO: 3.5 kDa, Spectrum Laboratories, Laguna Hills, CA) for 48 h with frequent exchange of fresh 10% ethanol solution to remove by-products. Finally, after dialyzing against DI water for 2 h, the dialyzed product was lyophilized, and the CSO-SA was received.

2.3. Physicochemical properties of CSO-SA

2.3.1. Substitute degree of amino groups (SD%) of CSO-SA

Substitute degree of amino groups (SD%) mean the number of SA groups per 100 amino groups of CSO, which was measured by TNBS method [27]. After 2 mL of 4% $NaHCO_3$ and 2 mL of 0.1% TNBS solution were added into 2 mL of CSO-SA solution with 125 μg/mL CSO-SA, the mixture was incubated for 2 h at 37 °C. Two milliliters of 2 N HCl solution were then added into mixture to neutralize the residue of $NaHCO_3$. The final reaction mixture was measured by UV spectroscopy (TU-1800PC, Beijing

Purkinje General Instrument Co., Ltd., China) setting the absorbance at 344 nm. The SD% of CSO-SA was calculated from calibration curve, which was obtained by CSO solution.

2.3.2. Critical micelle concentration (CMC) of CSO-SA

The critical micelle concentration (CMC) of CSO-SA was determined by fluorescence measurement using pyrene as a probe [28]. Fluorescence spectra was recorded on a fluorometer (F-2500, Hitachi Co., Japan) at room temperature. The excitation wavelength was 337 nm and the pyrene emission was monitored at a wavelength range of 360–450 nm. The concentration of CSO-SA solutions containing 5.93×10^{-7} M of pyrene was varied from 1.0×10^{-4} to 1.0 mg/mL. From the pyrene emission spectra, the intensity ratio of first peak (I_1, 374 nm) to third peak (I_3, 384 nm) was analyzed for the calculation of CMC.

2.3.3. Aggregation number of stearate groups per CSO-SA molecule

Aggregation number of stearate groups per CSO-SA molecule was estimated by steady-state fluorescence quenching method [29]. 0,0.25,0.5,0.75,1.0 mL of DPC ethanol solution (1.0×10^{-4} M) were added into different test tubes, respectively. After the test tubes were then maintained at 100 °C to volatilize solvent, 5 mL CSO-SA solution with 1.0 mg/mL CSO-SA concentration containing 5.93×10^{-7} M of pyrene was dropped into test tubes, respectively. Fluorescence spectra was recorded on a fluorometer (F-2500, Hitachi Co., Japan) at room temperature. The excitation wavelength, emission wavelength and slit openings were set at 337, 390, and 5 nm, respectively.

2.4. Preparation of crosslinked CSO-SA micelles

Crosslinked CSO-SA micelles were prepared by dropping glutaraldehyde into CSO-SA micelle solution with 1.0 mg/mL CAO-SA concentration, under mechanical stirring at room temperature [18]. The molar ratio of CSO-SA to glutaraldehyde was controlled at 1:1∼1:20 ($n_{\text{CSO-SA}}$:n_{glu}). The reaction time was controlled at 2, 4, 8 h, respectively. To terminate the crosslink of CSO-SA micelles by glutaraldehyde, glycine, and sodium bisulfate were selected as termination agent. After the CSO-SA micelles were reacted with glutaraldehyde for 2 h, the termination agent was added into the reaction mixture, and the termination reaction was conducted for 2, 4, or 8 h, respectively. The molar ratio of glutaraldehyde to termination agent was controlled at 1:4.

The size and zeta potential of CSO-SA and crosslinked CSO-SA micelles were determined by dynamic light scattering using a Zetasizer (3000HS, Malvern Instruments Ltd., UK).

2.5. Cell culture

A549 cells (human lung carcinoma epithelial cell (Alveolar type 2)), LLC cells (Lewis lung carcinoma cells), and SKOV3 cells (human ovarian cancer cell lines) were maintained in DMEM supplemented with 10% (v/v) FBS (fetal bovine serum) and penicillin/streptomycin (100 U mL^{-1}, 100 U mL^{-1}) at 37 °C and 5% CO_2. Cells were subcultured regularly using trypsin/EDTA.

2.6. Cellular uptake

2.6.1. Preparation of FITC-labeled CSO-SA micelles

FITC-labeled CSO-SA micelles (FITC-CSO-SA) were prepared by dropping ethanol solution of FITC into CSO-SA solution with 1.0 mg/mL CSO-SA. The molar ratio of CSO-SA to FITC was controlled at 1:4. Kept stirring for 24 h with 400 rpm at room temperature in aphotic environment, the reaction product was dialyzed against DI water using a dialysis membrane (MWCO: 3.5 kDa, Spectrum Laboratories, Laguna Hills, CA) for 24 h to remove the unreacted FITC. Then, the dialyzed product was lyophilized to receive FITC-CSO-SA.

2.6.2. Quantification of cellular uptake

A549, LLC, and SKOV3 cells were seeded at 1.0×10^5 mL^{-1} cells/well in a 24-well plate (Nalge Nunc International, Naperville, IL, USA) and grown for 24 h, respectively. After removing growth medium, 1 mL DMEM containing 50 μg/mL FITC–CSO-SA was added, and the cells were further incubated for 2, 4, 6, 8, and 12 h, respectively. After washing the cells with PBS three times, 50 μL trypsin PBS solution (2.5 mg/mL) was added, and incubated for 15 min. The cells were harvested by adding 1 ml PBS. The harvested cells were fragmented by freeze–thaw method [30] (All samples were frozen at −20 °C for 8 h, and tardily thawed at 25 °C, and the freeze-thaw cycles were recorded twice). Finally, the cell lysate was centrifuged at 10,000 rpm for 30 min and the supernatant was subjected to fluorescence assay by using fluorometer (F-4000, Hitachi Co., Japan) (excitation: 496 nm; emission: 522 nm).

The cellular uptakes of CSO-SA micelles were corrected to per microgram protein determined using the BCA protein assay kit. For the protein determination in cells, 20 μL cell lysate was added into 96-well plate, and 200 μL BCA working reagent was then added. The cell lysate was incubated at 37 °C for 30 min. UV absorbance at 570 nm of cell lysate was measured by a microplate reader (Bio-Rad, Model 680, USA). The protein concentration was calculated from calibration curve, which was obtained by using bovine serum albumin (BSA). The cellular uptake percentage of CSO-SA micelles was calculated from the following equation:

$$T_t(\%) = F_t/F_0 \times 100\%, \quad (1)$$

where T_t presents the cellular uptake percentage of CSO-SA micelles at t time; F_t is the ratio of fluorescence absorbance at t time to intracellular protein concentration at t time; F_0 is the ratio of fluorescence absorbance at 0 time to intracellular protein concentration at 0 time.

2.7. Preparation and characterization of doxorubicin-loaded CSO-SA micelles

2.7.1. Preparation of doxorubicin-loaded CSO-SA micelle

Doxorubicin base (DOX) was obtained by reaction of DOX·HCl with double mol triethylamine in DI water overnight, and used for the preparation of CSO-SA/DOX micelles. Ten milligrams of CSO-SA were dissolved in 2 mL DI water. Three hundred and fifty microliters of 1 mg/mL DOX–DMSO solution were added into CSO-SA solution under mechanical stirring at room temperature. After 4 h stirring, the mixture solution was dialyzed against DI water using a dialysis membrane (MWCO: 3.5 kDa, Spectrum Laboratories, Laguna Hills, CA) for 24 h. Dialyzed products were centrifuged at 4000 rpm for 10 min to remove precipitated drug during dialysis process. The supernatant was lyophilized to obtain doxorubicin-loaded CSO-SA micelle (CSO-SA/DOX).

2.7.2. Preparation of crosslinked doxorubicin-loaded CSO-SA micelle

The shell crosslinked CSO-SA/DOX was prepared by adding a rational amount of glutaraldehyde into CSO-SA/DOX solution with 1.0 mg/mL of CSO-SA concentration under mechanical stirring with 400 rpm at room temperature. The molar ratio of CSO-SA to glutaraldehyde ($n_{\text{CSO-SA}}$:n_{glu}) was 1:5, and the reaction time was 2 h. After the crosslink reaction, four molar times glycine against glutaraldehyde was added to terminate the reaction.

2.7.3. Determination of drug encapsulation efficiency and drug loading

The doxorubicin content was measured by fluorescence spectrophotometer. The excitation wavelength, emission wavelength and slit openings were set at 505, 565, and 5 nm, respectively.

The drug encapsulation efficiency and drug loading of CSO-SA/DOX and shell crosslinked CSO-SA/DOX were measured by centrifugal-ultrafiltration method. CSO-SA/DOX (0.5 mL) solution or shell crosslinked CSO-SA/DOX with 1.0 mg/mL of CSO-SA concentration was added into centrifugal-ultrafiltration tubes (Microcon YM-10, MWCO 3000, Millipore Co., USA), and centrifuged at 10,000 rpm for 10 min. The DOX amount (W) in ultrafiltrate was measured by fluorescence spectrophotometer. Another 0.5 mL CSO-SA/DOX solution with 1.0 mg/mL of CSO-SA concentration was diluted 100-fold by DMSO aqueous solution ($\text{DMSO}/\text{H}_2\text{O} = 9{:}1$, v/v) to dissociate the CSO-SA micelles. The DOX amount (W_0) in diluted solution was measured, and was considered as the total drug amount in 0.5 mL CSO-SA/DOX solution. The drug encapsulation efficiency (EE%) and drug loading of CSO-SA/DOX and shell crosslinked CSO-SA/DOX could be calculated by the following equations:

$$\text{EE}\% = (W_0 - W)/W_0 \times 100\% \quad (2)$$

$$\text{DL}\% = (W_0 - W)/(500 + W_0 - W) \times 100\%, \quad (3)$$

where W is the drug amount in ultrafiltrate; W_0 is the drug amount in 0.5 mL CSO-SA/DOX solution. The units were micrograms.

2.8. In vitro DOX release from the micelles

Phosphate-buffered saline (PBS), pH 7.2, was used as the dissolution medium in the in vitro DOX release tests from the micelles. The saturated solubility of DOX in pH 7.2 PBS was measured to be 76 μg/mL. One milliliter CSO-SA/DOX or shell crosslinked CSO-SA/DOX was added into a plastic tube containing 10 mL PBS (pH 7.2) solution. The plastic tube was then placed in an incubator shaker (HZ-8812S, Scientific and Educational Equipment plant, Tai Cang, China), which was maintained at 37 °C and shaken horizontally at 60 rpm. At predetermined time intervals, 0.4 mL sample was withdrawn, and was then centrifuged at 10,000 rpm for 10 min using a centrifugal-ultrafiltration tube (Microcon YM-10, MWCO 3000, Millipore Co., USA), and the drug concentration in ultrafiltrate was determined by fluorescence spectrophotometer. All drug release tests were performed thrice.

2.9. Cytotoxicity assay

Cytotoxicity of blank and DOX-loaded micelles against A549, LLC, and SKOV3 cells was evaluated by MTT assay [31]. The cells were seeded at 1.0×10^5 mL^{-1} cells/well in a 96-well plate (Nalge Nunc International, Naperville, IL, USA) and grown for 24 h. After removing growth medium, 100 μL DMEM containing different concentrations of CSO-SA, shell crosslinked CSO-SA, DOX, CSO-SA/DOX, and shell crosslinked CSO-SA/DOX was added, respectively. The cells were further incubated for 48 h. As a control the cells were incubated with DMEM for 48 h. The culture medium from each well was removed, and 100 μL DMEM and 10 μL MTT solution (5 mg/mL in PBS) were then added to each well. After 4 h further incubation, the culture medium were removed, and the formazan crystals in cells were solubilized with 100 μL DMSO for 15 min. The UV absorbance at 570 nm was measured using a microplate reader (Bio-Rad, Model 680, USA).

3. Results and discussion

3.1. Synthesis and characteristics of CSO-SA

Chitosan possessed two types of active groups to be modified by chemical reaction, one of them was amino group, and the others were C_6-OH and C_3-OH. Many of peptide and alkyl could be grafted to the chitosan molecule by coupling reaction to endow it with some potential characters. In this study, The CSO-SA was synthesized by the coupling reaction of SA and CSO. The SD% of CSO-SA was measured by TNBS method. TNBS is a substance that can react with the remaining primary amino residues on the CSO-SA molecules. The absorbance of purple reaction

production could be determined by a UV spectrophotometer. The SD% of CSO-SA was determined as 3.48%.

Due to the hydrophobic SA modification of water-soluble CSO molecules, the synthesized CSO-SA could self-aggregate to form micelles. The CMC of CSO-SA was assessed by fluorescence spectroscopy using pyrene as a probe. In the lower CSO-SA concentration, the fluorescence intensity and the ratio of the first peak to third peak (I_1/I_3) in the emission spectra of pyrene kept constant. As CSO-SA concentration increased to form micelles, the incorporation of pyrene into the micelles led to the increase of fluorescence intensity. The third peak in the emission spectra of pyrene increased significantly than that of first peak. As a result, the fluorescence intensity ratio of I_1/I_3 was reduced. The CSO-SA concentration causing the change of I_1/I_3 was the CMC value of CSO-SA. Fig. 1 shows the variation of fluorescence intensity ratio for I_1/I_3 against logarithm of CSO-SA concentration. The CMC value of CSO-SA was determined to be 0.035 mg/mL in DI water.

Aggregation number of hydrophobic microdomain per CSO-SA molecule was assessed by steady-state fluorescence quenching method. DPC was used as a quencher to quench pyrene fluorescence. The steady-state quenching date fit in quenching kinetics:

$$\ln(I_0/I) = [Q]/[M], \tag{4}$$

where I_0 and I are the fluorescence emission intensity, in the absence and presence of quencher, respectively. [Q] is the concentration of the quencher, and [M] is the concentration of hydrophobic stearate microdomains in micelles. So, the number of stearate groups per hydrophobic microdomain can be determined by Eq. (5):

$$n_{SA} = [SA]/[M], \tag{5}$$

where n_{SA} is the number of stearate groups per hydrophobic microdomain, and [SA] is the concentration of SA. Thus, the aggregation number of hydrophobic microdomain per CSO-SA molecule can be calculated by the following equation:

$$AN = n_{NH_2} \times SD/n_{SA}, \tag{6}$$

where n_{NH_2} is the total number of amino groups per CSO-SA molecule.

Fig. 2 shows the plot of $\ln(I_0/I)$ of pyrene fluorescence against DPC concentration in the presence of 1.0 mg/mLCSO-SA. From the linear relationship between $\ln(I_0/I)$ and DPC concentration, the [M] was obtained. Based on Eqs. (5) and (6), the aggregation number of hydrophobic stearate microdomain per CSO-SA molecule was calculated as 2.8.

3.2. Preparation and characteristics of shell crosslinked CSO-SA micelles

The shell of CSO-SA micelles was crosslinked by glutaraldehyde *via* Schiff's reaction in neutral medium. The effects of glutaraldehyde amount and reaction time on micelle size are shown in Fig. 3. Fig. 3(b) is the magnified figure for the reaction time between 0 and 4 h in Fig. 3(a). From Fig. 3, it is clear that the higher glutaraldehyde amount ($n_{CSO\text{-}SA}$:n_{glu} = 1:20) induced the size increase during reaction due to the Schiff's reaction between micelles. In the lower glutaraldehyde amount ($n_{CSO\text{-}SA}$:n_{glu} = 1:2.5), no obvious size change was found in 4 h, and significant size increase was observed after 4 h, because of the slower Schiff's reaction. In the middle glutaraldehyde amount ($n_{CSO\text{-}SA}$:n_{glu} = 1:5, 1:10, 1:15), the particle size reduced with reaction time in 8 h, and increased after 8 h. The decreased size in 8 h might have resulted from the crosslink between CSO-SA molecules intra-micelle, which led to a tight structure of micelle. The increased size after 8 h was due to the crosslink between micelles. Considering above results, the glutaraldehyde amount and reaction time were fixed at $n_{CSO\text{-}SA}$:n_{glu} = 1:5 and 2 h, respectively. As shown in Table 1, after the shell crosslinking reaction, the micelle size was slightly reduced, and the zeta potential was decreased from 57.1 ± 1.5 to 34.2 ± 0.5 mV. Increasing the glutaraldehyde amount and reaction time led to the zeta potential of micelles below 30 mV (data not shown).

As shown in Fig. 3(a), the prolonged reaction time could cause a bigger change in micelle size. To prevent further

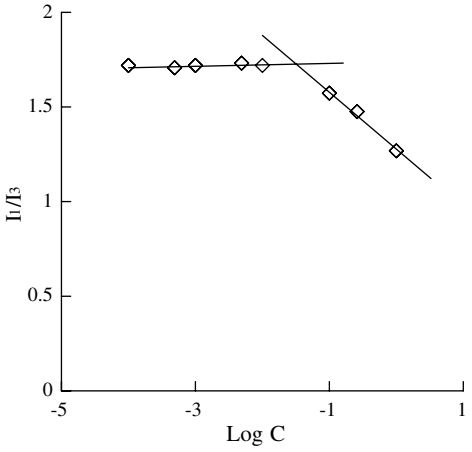

Fig. 1. Variation of fluorescence intensity ratio for I_1/I_3 against logarithm of CSO-SA concentration.

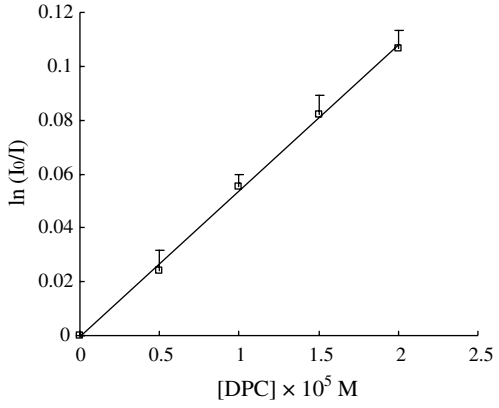

Fig. 2. Plot of $\ln(I_0/I)$ of pyrene fluorescence against DPC concentration in the presence of 1.0 mg/mL CSO-SA.

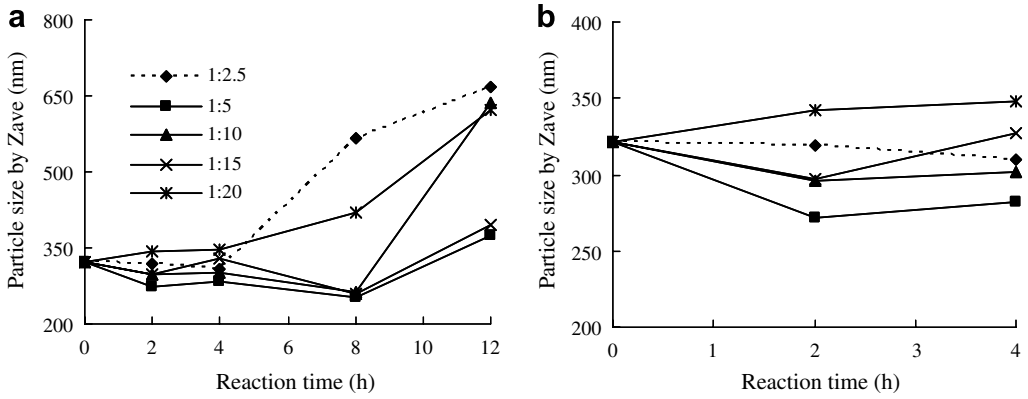

Fig. 3. Effects of glutaraldehyde amount and reaction time on the micelle size, (b) is the magnified figure for the reaction time between 0 and 4 h in (a).

Table 1
Physicochemical properties of CSO-SA micelles, shell crosslinked CSO-SA micells, CSO-SA/DOX, and shell crosslinked CSO-SA/DOX

Sample	Size by Zave (nm)	Size by number (nm)	PI[a]	Zeta potential (mV)	EE (%)	DL (%)
CSO-SA	322.3	35.0	0.632	57.1 ± 1.5	–	–
Crosslinked CSO-SA	272.0	25.4	0.530	34.2 ± 0.5	–	–
CSO-SA/DOX	355.0	40.7	0.560	69.1 ± 0.3	93.7 ± 0.60	1.67
Crosslinked CSO-SA/DOX	305.3	30.4	0.622	51.8 ± 0.7	93.4 ± 1.71	1.67

[a] PI, Polydispersity Index.

crosslinking reaction at the later stage, the termination reagent was used to stop crosslinking reaction. Herein, sodium bisulfate and glycine were selected termination reagent. Fig. 4 shows the micelle size change after the addition of termination reagent. It could be found that the use of sodium bisulfate led to slight increase of micelle size. It might have resulted from the salt effect of sodium bisulfate, which could disturb the stability of micelles. The use of glycine could maintain the micelle size, and was selected as termination reagent.

3.3. Cellular uptake of CSO-SA micelles and shell crosslinked CSO-SA micelles

Using A549, LLC, and SKOV3 cells as model tumor cells, the cellular uptakes of CSO-SA micelles and shell crosslinked CSO-SA micelles were carried out. FITC labeled CSO-SA micelles (FITC-CSO-SA) were prepared by the chemical reaction between amino groups of CSO-SA and isothiocyanate group of FITC molecule [32]. Fig. 5 shows the cellular uptake percentage of CSO-SA micelles and shell crosslinked CSO-SA micelles in A549, LLC, and SKOV3 cells against incubation time. It was found the cellular uptakes of CSO-SA micelles and shell crosslinked CSO-SA micelles were increased with incubation time, and the cellular uptake percentage of micelles in LLC (b), and SKOV3 cells (c) was higher than that of micelles in A549 cells (a). After 12 h, the cellular uptake percentage of CSO-SA micelles in A549 cells was about 20.9%. Meanwhile, cellular uptake percentage in LLC and SKOV3 cells was 49.1% and 55.0%, respectively. It was also found that there were no significantly differences in cellular uptake percentage between CSO-SA micelle and shell crosslinked micelle. After the shell crosslinking, the zeta potential of CSO-SA micelles decreased from 57.1 to 34.2 mV (Table 1). The reduced surface charge might weaken the interaction between positive charged CSO-SA micelles and negative charged cell surface, and hence decrease the cellular uptake [33]. However, the decreased size of shell crosslinked CSO-SA could enhance the cellular uptake of micelles [34].

3.4. Preparation and characterization of doxorubicin-loaded micelles

Table 1 shows the properties of CSO-SA and CSO-SA/DOX before and after shell crosslinking. After the loading of drug, the size and zeta potential of CSO-SA/DOX were

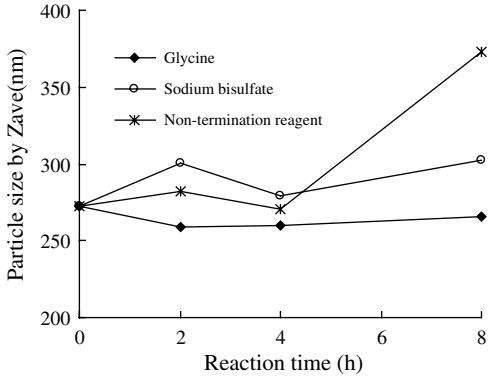

Fig. 4. Effects of sodium bisulfate and glycine as termination reagent on the micelle size.

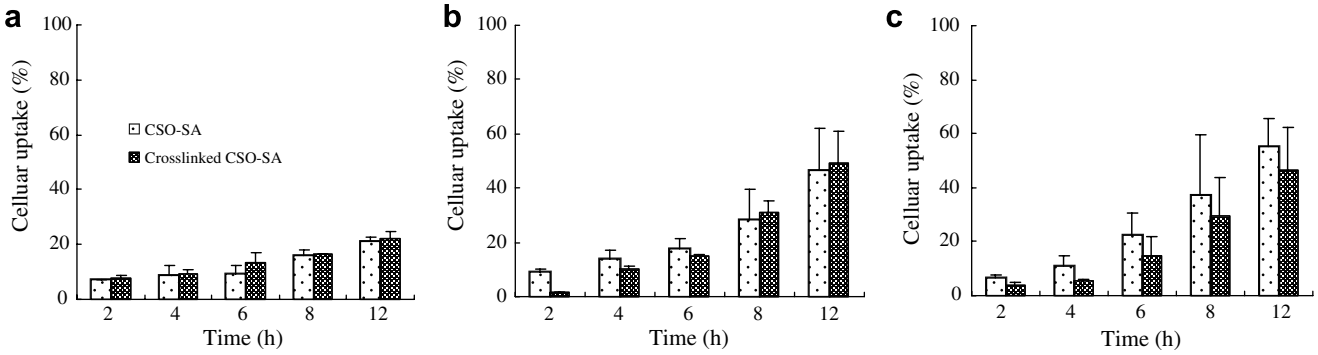

Fig. 5. Cellular uptake percentage of CSO-SA micelles and shell crosslinked CSO-SA micelles in A549, LLC, and SKOV3 cells against incubation time. (a) A549, (b) LLC, and (c) SKOV3.

slightly increased. The increase in zeta potential might have been caused by the positive charge of DOX. The EE (%) results of drug-loaded micelle and its crosslinked micelle in Table 1 indicate that the loading of DOX in the CSO-SA micelles could reach higher EE (%), and that the shell crosslinking of CSO-SA micelles does not affect the EE (%). DL (%) of CSO-SA/DOX was just about half of charged drug content, which might be due to the drug loss in dialysis process.

In vitro drug release from DOX-loaded micelles was carried out using pH 7.2 PBS as dissolution medium. Fig. 6 shows the drug release profiles from CSO-SA/DOX and shell crosslinked CSO-SA/DOX. It was clear that the released percentage of drug at 0 time was significantly decreased by the shell crosslinking of CSO-SA micelles. At 0 time, 31.0% drug was released from CSO-SA/DOX, meanwhile, only 22.4% drug was released from shell crosslinked CSO-SA/DOX. This result means the shell crosslinking of CSO-SA/DOX could reduce the dissociation of CSO-SA micelles during diluting process. Fig. 6 also shows that the drug release from shell crosslinked CSO-SA/DOX was much slower than from unmodified micelles. About 62.5% drug was released from unmodified micelle at 2 h, but only 45.4% drug was released from shell crosslinked micelle at the same time. Unmodified micelles showed nearly complete release at 12 h, but shell crosslinked micelles just released 67.7% at 12 h, 77.8% at 24 h. The possible reason was the tight structure of shell crosslinked CSO-SA micelle.

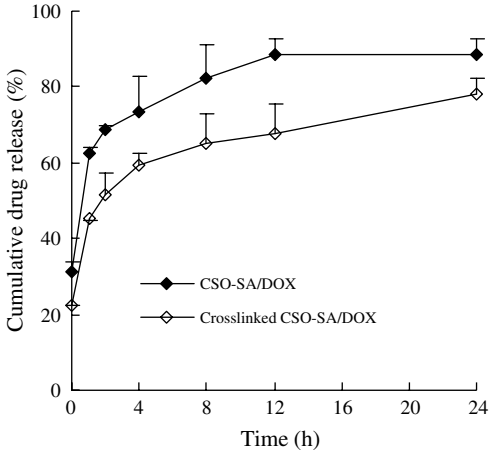

Fig. 6. Drug release profiles from CSO-SA/DOX and shell crosslinked CSO-SA/DOX in PBS (pH 7.2) solution.

3.5. Cytotoxicity of CSO-SA/DOX and shell crosslinked CSO-SA/DOX

The cellular growth inhibition of CSO-SA, crosslinked micelles, free drug, CSO-SA/DOX, and shell crosslinked CSO-SA/DOX against material or drug concentration is shown in Fig. 7, and the calculated 50% cellular growth inhibition (IC_{50}) of CSO-SA, crosslinked micelles, free drug, CSO-SA/DOX and shell crosslinked CSO-SA/DOX against A549, LLC, and SKOV3 cells is listed in Table 2. From Table 2, it could be seen that the IC_{50} value of CSO-SA on A549 cells was twice that on LLC and SKOV3 cells. The lower IC_{50} value of CSO-SA on LLC and SKOV3 cells might have originated from the faster cellular uptake of CSO-SA micelles on LLC and SKOV3 cells. After 12 h, the cellular uptake percentage of CSO-SA micelles on LLC and SKOV3 cells was above twice that on A549 cells. Comparing with the IC_{50} value of CSO-SA, no obvious change was found in shell crosslinked CSO-SA micelles. It means the cytotoxicity of glutaraldehyde could be removed by addition of termination reagent.

DOX is one of the most useful antibiotics with a wide spectrum of activity against malignancy, such as, lung cancer, haematological malignancies, breast cancer, and so on. Although it is also used for treating other tumors like ovarian carcinoma, liver cancer, and stomach cancer, it is not the first selection in the clinic because of its lower sensitivity against these cells. The results indicate that the IC_{50} value of free DOX on A549, LLC, and SKOV3 cells was 1.40, 1.08 and 3.24 μg/mL. It means that DOX is more sensitive against lung cancer than ovarian carcinoma cell. When DOX molecules were encapsulated into the micelles of CSO-SA, the cytotoxicity of CSO-SA/DOX was much greater than that of free DOX. The IC_{50} values reduced above twice. It might be attributed to the internalization of CSO-SA micelles, which could transport more drug into

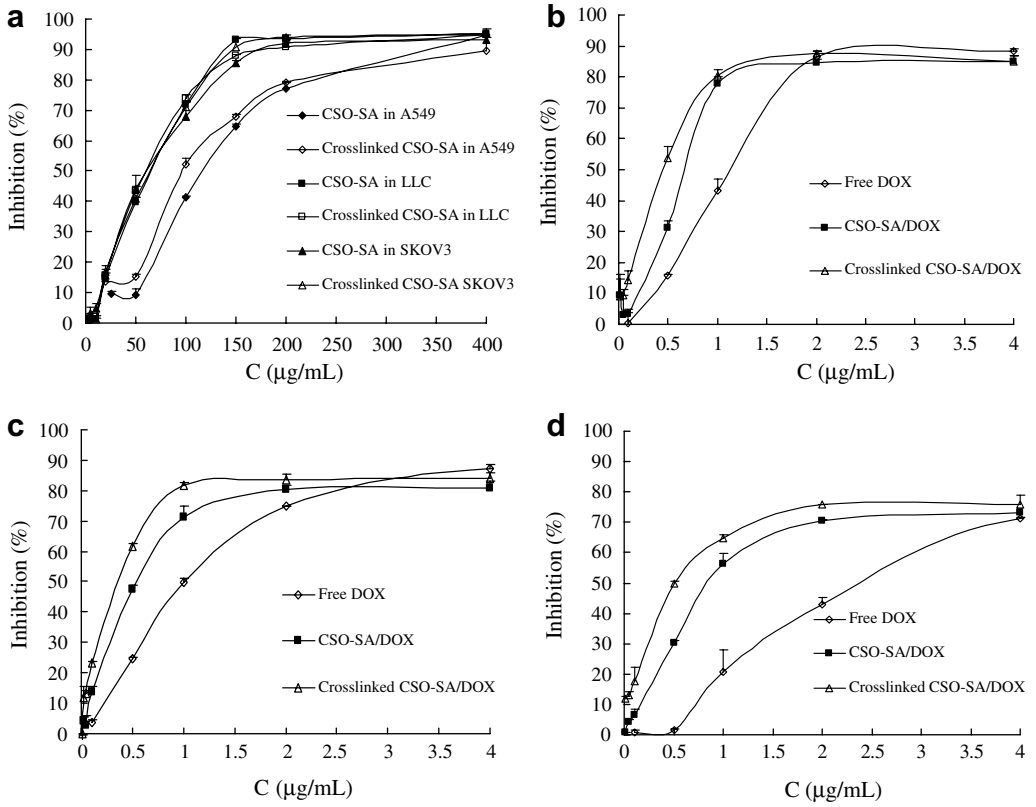

Fig. 7. Plots of cellular growth inhibition against material or drug concentration (C, μg/ml). (a) CSO-SA micelle and shell crosslinked CSO-SA micelle on A549, LLC, and SKOV3 cell lines; (b) DOX, CSO-SA/DOX, and crosslinked CSO-SA/DOX on A549 cells; (c) DOX, CSO-SA/DOX, and crosslinked CSO-SA/DOX on LLC cells; and (d) DOX, CSO-SA/DOX, and crosslinked CSO-SA/DOX on SKOV3 cells.

Table 2
IC_{50} values of CSO-SA micelles, shell crosslinked CSO-SA mic ells, CSO-SA/DOX, and shell crosslinked CSO-SA/DOX against A549, LLC, and SKOV3 cell lines

Sample	IC_{50} (μg/mL)			Reduced fold		
	A549	LLC	SKOV3	A549	LLC	SKOV3
CSO-SA	95.2 ± 3.1	54.3 ± 2.0	53.4 ± 0.2	–	–	–
Crosslinked CSO-SA	107.1 ± 2.8	54.7 ± 1.0	50.9 ± 0.7	–	–	–
Free DOX	1.40 ± 0.23	1.08 ± 0.06	3.24 ± 0.05	–	–	–
CSO-SA/DOX	0.65 ± 0.01	0.4 ± 0.03	0.7 ± 0.02	2.2	2.7	4.6
Crosslinked CSO-SA/DOX	0.30 ± 0.08	0.24 ± 0.01	0.39 ± 0.01	4.7	4.5	8.3

cells [28]. In addition, the reduced fold of IC_{50} of CSO-SA/DOX against SKOV3 was higher than that on lung cancer cells. It might be due to the poor cellular uptake of DOX in SKOV3 cells. Notice, the IC_{50} values of CSO-SA/DOX on three cells were almost same. It means that the CSO-SA micelles could significantly improve the cytotoxicity in drug-insensitive tumor cells.

Moreover, cytotoxicity of crosslinked CSO-SA/DOX was much greater than that of CSO-SA/DOX. It might be attributed to the significant reduction of drug leakage before DOX-loaded micelles were internalized into cells. Considering the results of drug release in vitro, the shell crosslinking of CSO-SA/DOX did not affect the drug release after the shell crosslinked CSO-SA/DOX were internalized into cells. The cytotoxicity results indicated that the shell crosslinking of CSO-SA/DOX could further increase the drug concentration in cells and the antitumor efficacy.

4. Conclusions

An amphiphilic stearic acid-grafted chitosan oligosaccharide was synthesized, and utilized to fabricate micelles for the delivery of antitumor drug. Due to the spatial structure with multi-hydrophobic core, the CSO-SA micelles could rapidly internalized into tumor cells, and showed different cellular uptake abilities in different tumor cell lines. The cellular uptakes in LLC and SKOV3 cells were higher than that in A549 cells. The shell crosslinking of CSO-SA micelles by glutaraldehyde did not significantly change the properties of CSO-SA micelles and CSO-SA/DOX, such as the micelle size, cellular uptake ability. However the shell crosslinking

of CSO-SA/DOX could highly decrease the burst drug release from CSO-SA micelles. The cytotoxicities of DOX against tumor cells were increased by the encapsulation of CSO-SA micelles, especially in DOX-insensitive tumor cell lines. The shell crosslinked CSO-SA/DOX could further enhance the cytotoxicity of DOX due to the reduced drug loss in diluting process.

Acknowledgments

We thank the financial supports of the National Nature Science Foundation of China under Contract Nos. 30472101 and 30672552, and the Nature Science Foundation of Zhejiang province under Contract No. M303817.

References

[1] D.J. Bharali, S.K. Sahoo, S. Mozumdar, A. Maitra, Cross-linked polyvinylpyrrolidone nanoparticles: a potential carrier for hydrophilic drugs, J. Colloid Interf. Sci. 258 (2003) 415–423.
[2] K. Letchford, H. Burt, A review of the formation and classification of amphiphilic block copolymer nanoparticulate structures: micelles, nanospheres, nanocapsules and polymersomes, Eur. J. Pharm. Biopharm. 65 (2007) 259–269.
[3] D.A. Chiappetta, A. Sosnik, Poly(ethylene oxide)–poly(propylene oxide) block copolymer micelles as drug delivery agents: improved hydrosolubility, stability and bioavailability of drugs, Eur. J. Pharm. Biopharm. 66 (2007) 303–317.
[4] Z. Sezgin, N. Yüksel, T. Baykara, Preparation and characterization of polymeric micelles for solubilization of poorly soluble anticancer drugs, Eur. J. Pharm. Biopharm. 64 (2006) 261–268.
[5] M.C. Jones, J.C. Leroux, Polymeric micelles – a new generation of colloidal drug carriers, Eur. J. Pharm. Biopharm. 48 (1999) 101–111.
[6] H. Maeda, The enhanced permeability and retention (EPR) effect in tumor vasculature: the key role of tumor-selective macromolecular drug targeting, Adv. Enzyme Regul. 41 (2001) 189–207.
[7] H. Maeda, J. Wu, T. Sawa, Y. Matsumura, K. Hori, Tumor vascular permeability and the EPR effect in macromolecular therapeutics: a review, J. Control. Release 65 (2000) 271–284.
[8] G. Zuccari, R. Carosio, A. Fini, P.G. Montaldo, I. Orienti, Modified polyvinylalcohol for encapsulation of all-trans-retinoic acid in polymeric micelles, J. Control. Release 103 (2005) 369–380.
[9] K.B. Thurmond, H.Y. Huang, C.G. Clark, T. Kowalewski, K.L. Wooley, Shell cross-linked polymer micelles: stabilized assemblies with great versatility and potential, Colloid Surf. B-Biointerfaces 16 (1999) 45–54.
[10] K. Kataoka, T. Matsumoto, M. Yokoyama, T. Okano, Y. Sakurai, S. Fukushima, K. Okamoto, G.S. Kwon, Doxorubicin-loaded poly (ethylene glycol)–poly (β-benzyl-L-aspartate) copolymer micelles: their pharmaceutical Characteristics and biological significance, J. Control. Release 64 (2000) 143–153.
[11] S. Bontha, A.V. Kabanov, T.K. Bronich, Polymer micelles with cross-linked ionic cores for delivery of anticancer drugs, J. Control. Release 114 (2006) 163–174.
[12] T. Kean, S. Roth, M. Thanou, Trimethylated chitosans as non-viral gene delivery vectors: cytotoxicity and transfection efficiency, J. Control. Release 103 (2005) 643–653.
[13] P. Opanasopit, T. Ngawhirunpat, A. Chaidedgumjorn, T. Rojanarata, A. Apirakaramwong, S. Phongying, C. Choochottiros, S. Chirachanchai, Incorporation of camptothecin into *N*-phthaloyl chitosan-γ-mPEG self-assembly micellar system, Eur. J. Pharm. Biopharm. 64 (2006) 269–276.
[14] C. Zhang, P. Qineng, H. Zhang, Self-assembly and characterization of paclitaxel-loaded *N*-octyl-*O*-sulfate chitosan micellar system, Colloid Surf. B-Biointerfaces 39 (2004) 69–75.
[15] Z. Aipinga, J.H. Liu, W.H. Ye, Effective loading and controlled release of camptothecin by *O*-carboxymethylchitosan aggregates, Carbohydr. Polym. 63 (2006) 89–96.
[16] Y.Q. Ye, F.Q. Hu, H. Yuan, Preparation and characterization of stearic acid-grafted chitosan oligosaccharide polymeric micelles, Acta Pharm. Sin. 6 (2004) 467–471.
[17] F.Q. Hu, M.D. Zhao, A novel chitosan oligosaccharide–stearic acid micelles for gene delivery: properties and in vitro transfection studies, Int. J. Pharm. 315 (2006) 158–166.
[18] F.Q. Hu, G.F. Ren, H. Yuan, Y.Z. Du, S. Zeng, Shell cross-linked stearic acid grafted chitosan oligosaccharide self-aggregated micelles for controlled release of paclitaxel, Colloid Surf. B-Biointerfaces 50 (2006) 97–103.
[19] J. You, F.Q. Hu, Y.Z. Du, H. Yuan, Polymeric micelles with glycolipid-like structure and multiple hydrophobic domains for mediating molecular-target delivery of paclitaxel, Biomacromolecules 8 (2007) 2450–2456.
[20] A. Nori, J. Kopecek, Intracellular targeting of polymer-bound drugs for cancer chemotherapy, Adv. Drug Deliv. Rev. 57 (2005) 609–636.
[21] G. Toffoli, C. Cernigoi, A. Russo, A. Gallo, M. Bagnoli, M. Boiocchi, Overexpression of folate binding protein in ovarian cancers, Int. J. Cancer 74 (1997) 193–198.
[22] Y.J. Lu, P.S. Low, Immunotherapy of folate receptor-expressing tumors: review of recent advances and future prospects, J. Control. Release 91 (2003) 17–29.
[23] G.Y. Lee, K. Park, S.Y. Kim, Y. Byun, MMPs-specific PEGylated peptide–DOX conjugate micelles that can contain free doxorubicin, Eur. J. Pharm. Biopharm. 67 (2007) 646–654.
[24] L.Y. Qiu, Y.H. Bae, Self-assembled polyethylenimine-graft-poly (ε-caprolactone) micelles as potential dual carriers of genes and anticancer drugs, Biomaterials, doi:10.1016/j.biomaterials.2007.05.035.
[25] S.Q. Liu, Y.W. Tong, Y.Y. Yang, Incorporation and in vitro release of doxorubicin in thermally sensitive micelles made from poly(*N*-isopropylacrylamide-co-*N*,*N*-dimethylacrylamide)-β-poly(D,L-lactide-co-glycolide) with varying compositions, Biomaterials 26 (2005) 5064–5074.
[26] H.G. Schild, D.A. Tirrell, Microheterogenous solutions of amphiphilic copolymers of *N*-isopropylacrylamide. An investigation via fluorescence methods, Langmuir 7 (1991) 1319–1324.
[27] A.B. Schnurch, M.E. Krajicek, Mucoadhesive polymers as platforms for peroral peptide delivery and absorption: synthesis and evaluation of different chitosan–EDTA conjugates, J. Control. Release 50 (1998) 215–223.
[28] S.Q. Liu, N. Wiradharma, S.J. Gao, Y.W. Tong, Y.Y. Yang, Bifunctional micelles self-assembled from a folate-conjugated block copolymer for targeted intracellular delivery of anticancer drugs, Biomaterials 28 (2007) 1423–1433.
[29] K.Y. Lee, W.H. Jo, Structural determination and interior polarity of self-aggregates prepared from deoxycholic acid-modified chitosan in water, Macromolecules 31 (1998) 378–383.
[30] J.D. Morris, J.M. Fernandez, A.M. Chapa, L.R. Gentry, K.E. Thorn, T.M. Weick, Effects of sample handling, processing, storage, and hemolysis on measurement of key energy metabolites in ovine blood, Small Ruminant Res. 43 (2002) 157–166.
[31] Y.D. Zhang, Z.Y. Hu, M.Y. Ye, Y.F. Pan, J.J. Chen, Y.L. Luo, Y.Q. Zhang, L.X. He, J.W. Wang, Effect of poly(ethylene glycol)-block-polylactide micelles on hepatic cells of mouse: low cytotoxicity, but efflux of the micelles by ATP-binding cassette transporters, Eur. J. Pharm. Biopharm. 66 (2007) 268–280.
[32] Y.J. Son, J.S. Jang, Y.W. Cho, H. Chung, R.W. Park, I.C. Kwon, I.S. Kim, J.Y. Park, S.B. Seo, C.R. Park, S.Y. Jeong, Biodistribution and anti-tumor efficacy of doxorubicin loaded glycol–chitosan nanoaggregates by EPR effect, J. Control. Release 91 (2003) 135–145.
[33] S. Mao, O. Germershaus, D. Fischer, T. Linn, R. Schnepf, T. Kissel, Uptake and transport of PEG-graft–trimethyl-chitosan copolymer–insulin nanocomplexes by epithelial cells, Pharm. Res. 22 (2005) 2058–2068.
[34] Y. Hu, J.W. Xie, Y.W. Tong, C.H. Wang, Effect of PEG conformation and particle size on the cellular uptake efficiency of nanoparticles with the HepG2 cells, J. Control. Release 118 (2007) 7–17.